Theoretical growth rate of microalgae under high/low-flashing light

Ignacio Fierro, Liu-Di Lu, Olivier Bernard

Theoretical growth rate of microalgae under high/low-flashing light

J. Ignacio Fierro U.[1*], Liu-Di Lu[2] and Olivier Bernard[1]

[1*]BIOCORE Project-Team, Inria Sophia Antipolis Méditerranée, Université Nice Côte d'Azur, 2004, Route des Lucioles - BP 93, Sophia-Antipolis, 06902, France.
[2]Section de mathématiques, Université de Genève, Rue du Conseil-Général 7-9, Genève, 1205, Switzerland.

*Corresponding author(s). E-mail(s): joel-ignacio.fierro-ulloa@inria.fr;
Contributing authors: liudi.lu@unige.ch; olivier.bernard@inria.fr;

Abstract

Dynamic light regimes strongly impact microalgal photosynthesis efficiency. Finding the optimal way to supply light is then a tricky problem, especially when the growth rate is inhibited by overexposition to light and, at the same time, there is a lack of light in the deepest part of the culture. In this paper, we use the Han model to study the theoretical microalgal growth rate by applying periodically two different light intensities. Two approaches are considered depending on the period of the light pattern. For a large light period, we demonstrate that the average photosynthetic rate can be improved under some conditions. Moreover, we can also enhance the growth rate at steady state as given by the PI-curve. Although, these conditions change through the depth of a bioreactor. This theoretical improvement in the range of 10 to 15% is due to a recovery of photoinhibited cells during the high irradiance phase. We give a minimal value of the duty cycle for which the optimal irradiance is perceived by the algae culture under flashing light regime.

Keywords: Microalgae, Flashing light, Growth rate, Han model

MSC Classification: 34A05 , 34A30 , 34C25

1 Introduction

Algal biomass has a great potential for the production of novel food, feed, pharmaceuticals and cosmetics (Milledge, 2011). This approach has also been actively studied for wastewater treatment, with the advantage of recycling nitrogen and phosphorus for producing commodities (Balamurugan et al, 2021). Algal growth is influenced by different factors such as temperature, light, nutrients, pH, etc. Among them, light is a crucial factor for photosynthesis that fuels CO_2 uptake and further microalgal growth. In this work, we explore the consequences of the Han model (Han, 2002) for cultures where light is the limiting factor. Han's model describes the photosynthesis process by representing the reaction center dynamics through three states, one of them corresponding to photoinhibition. This model has been used by several authors who demonstrated that it can properly predict the growth rate of cultures submitted to a periodic light/dark alternation (Béchet et al, 2013; Baklouti et al, 2006; Pozzobon and Perre, 2018). Moreover, it has been coupled with acclimation (Nikolaou et al, 2016), and chlorophyll fluorescence models (Nikolaou et al, 2015).

Photoinhibition is a phenomenon where photosynthesis rate decreases at high irradiance. There are several reasons for photoinhibition (Raven, 2011), such as oxidative stress resulting from reactive oxygen species (ROS) as inevitable by-products of photosynthesis, but also severe inhibition of the activity of photosystem II (PSII) by damaging (photodamage) essential proteins in PSII such as the D1 protein (Prasil et al, 1992). This so called photoinhibition of PSII induces a high turnover rate of D1 protein for repairing photosystem II (PSII) after being damaged by photoinhibitory irradiance. Then, photoinhibition is controlled by balancing between damage to and recovery of D1 protein.

Flashing light is often considered as a method to reduce photoinhibition and to increase the productivity in photobioreactors. This consists of a periodic succession of light and dark phases. There is a lot of research on the benefit of providing light through flashes (Abu-Ghosh et al, 2016; Fernández-Sevilla et al, 2018; Abu-Ghosh et al, 2015a; Schulze et al, 2020). The flashing light, however, rarely produces an enhancement on the algal production in comparison with the constant light of the same average irradiance (Abu-Ghosh et al, 2015b). In the current work, we consider a different light regime, namely the high/low flashing light regime. The microalgae culture is considered to be exposed to a periodic succession of high irradiance followed by lower irradiance. This light regime is more representative of real conditions in dense cultures of microalgae where light is absorbed and scattered by the algae culture and cannot penetrate deeply into the liquid medium (Stramski et al, 2002). As a consequence, cells oscillate randomly between the surface layer at high irradiance and the deeper layers at lower irradiance (Demory et al, 2018).

The aim of this paper is to go beyond the flashing light pattern to understand how a high/low flashing light affects the growth rate of microalgae.

To address this question, we reduce the Han model into only one differential equation. This simplification depends on the timescale of the period of the high/low flashing light configuration. We differentiate two cases regarding large and small timescales. Meanwhile, we provide an approximation of the average growth rate for each case, and compare the solutions of the simplified models with the exact solution of the system. With these simplified models, we prove that the solution of this system, considering the high/low flashing light configuration, converge to a periodical solution, and we study their properties.

We show that the average growth rate under a high/low flashing light regime can be greater than the growth under constant light regime with the same average irradiance. We also prove theoretically that for high frequencies (or short period of the light pattern) the growth rate under the high/low flashing light regime is equal to the growth rate under the constant light regime. We consider the local optical depth concept defined in (Bernard and Lu, 2021) for our analysis to condense the effect of the depth and biomass in the light attenuation.

This paper is organized as follows. In Section 2, we present the growth model and the light setting. In Section 3, we analyze what happen in the large period approach which will be called *Large-T model* and how this case can improve the growth rate comparing to the continuous light regime. In Section 4, we study the small period approach called *Small-T model*, and we give an interval in which the algae culture perceives the optimal light if we consider the flashing light configuration. Section 5 justifies the approximations made in the previous sections. Finally, in Section 6, we test numerically the results.

2 Description of the model

2.1 Han model

In the Han model (Han, 2002), reaction centers of PSII can take three states: open or reactive (state A), closed or activated (state B) and inhibited (state C). After absorbing photons, reaction centers move from state A to B at a rate proportional to σI, where σ is the *effective cross section* of the reaction center and I is the irradiance. The minimal time required for an electron to transfer from water on the donor side of PSII to terminal electron acceptors is called *turnover time* and denoted by τ, so that τ^{-1} corresponds to the rate of state B passing to state A. Excessive light absorption leads to photoinhibition of the PSII (C state) at a rate $k_d\sigma I$ and has a recovery rate k_r. Figure 1a presents the relation between these three states. The dynamics of PSIIs at the three states can be described by the following differential equations, which describe

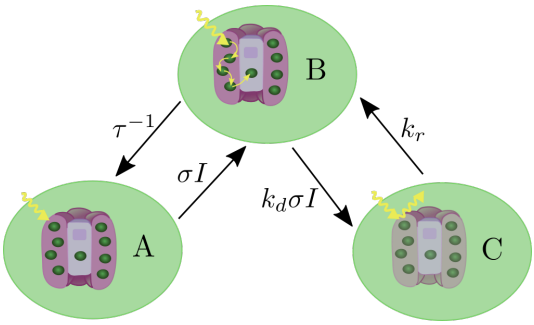

(a) Illustration of the Han Model.

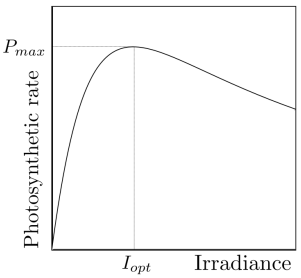

(b) PI-curve when A is at steady state following the Haldane description given by (4)

the proportion of each state:

$$\begin{aligned} \frac{\mathrm{d}A}{\mathrm{d}t} &= -I\sigma A + \frac{B}{\tau}, \\ \frac{\mathrm{d}B}{\mathrm{d}t} &= I\sigma A - \frac{B}{\tau} + k_r C - k_d \sigma I B, \\ \frac{\mathrm{d}C}{\mathrm{d}t} &= -k_r C + k_d \sigma I B, \end{aligned} \tag{1}$$

and these three states satisfy:

$$A + B + C = 1. \tag{2}$$

Then system (1) is defined in the domain $\{(A, B, C) \in [0, 1]^3 : A+B+C = 1\}$, which is well defined due to the fact that $\frac{\mathrm{d}}{\mathrm{d}t}(A+B+C) = 0$. On the other hand, growth rate μ depends entirely on the irradiance that the algae perceived, and it is proportional to $I\sigma A$:

$$\mu \coloneqq K\sigma I A, \tag{3}$$

where K corresponds to the growth rate coefficient.

At steady state of system (1), the growth rate given by the Han model, for a constant irradiance I can be computed explicitly by

$$\mu_S(I) \coloneqq \frac{K\sigma I}{1 + \tau\sigma I + \frac{k_d}{k_r}\tau(\sigma I)^2}. \tag{4}$$

This formulation corresponds to a Haldane description of the PI-curve accounting for photoinhibition. In Figure 1b, we present a generic form of the PI-curve

with this description. The maximum of this function is given by

$$\mu_{\max} := \frac{K}{\tau + 2\sqrt{\frac{k_d}{k_r}\tau}}, \tag{5}$$

which is achieved with the irradiance I_{opt} given by

$$I_{\text{opt}} := \frac{1}{\sigma\sqrt{\frac{k_d}{k_r}\tau}}. \tag{6}$$

The details of the above computation and the link between (4) and the Haldane description can be found for instance in (Lu, 2021, Proposition 1.2.1).

Using Equation (2), we can eliminate B to reduce the system (1) into two equations:

$$\frac{\mathrm{d}}{\mathrm{d}t}\begin{pmatrix} A \\ C \end{pmatrix} = \begin{pmatrix} 1 & 0 \\ 0 & k_d \end{pmatrix}\left[-\begin{pmatrix} \sigma I + \frac{1}{\tau} & \frac{1}{\tau} \\ \sigma I & \sigma I + \frac{k_r}{k_d} \end{pmatrix}\begin{pmatrix} A \\ C \end{pmatrix} + \begin{pmatrix} \frac{1}{\tau} \\ \sigma I \end{pmatrix}\right], \tag{7}$$

which can be also rewritten as

$$\frac{\mathrm{d}}{\mathrm{d}t}\begin{pmatrix} A \\ C \end{pmatrix} = -M(I)\begin{pmatrix} A \\ C \end{pmatrix} + N(I),$$

where

$$M(I) := \begin{pmatrix} \sigma I + \frac{1}{\tau} & \frac{1}{\tau} \\ k_d\sigma I & k_d\sigma I + k_r \end{pmatrix}, \quad N(I) := \begin{pmatrix} \frac{1}{\tau} \\ k_d\sigma I \end{pmatrix}. \tag{8}$$

For every value of $I \in \mathbb{R}^+$, the matrix $-M(I)$ is Hurwitz (see Appendix A.5) and invertible. Then $M^{-1}(I)N$ is the only asymptotically stable equilibrium, which can be computed explicitly by

$$\begin{pmatrix} A^* \\ C^* \end{pmatrix} := M^{-1}(I)N(I) = \frac{1}{1 + \tau\sigma I + \frac{k_d}{k_r}\tau(\sigma I)^2}\begin{pmatrix} 1 \\ \tau\frac{k_d}{k_r}(\sigma I)^2 \end{pmatrix},$$

with A^*, C^* the steady state of A, C. Using the definition of the growth rate (3), one re-finds (4) by multiplying A^* with $K\sigma I$.

2.2 Light regimes and the two simplified models

2.2.1 Definitions

Let us consider two light regimes, namely the constant regime and the high/low-flashing light regime. For the constant light regime, the reactor receives a constant irradiance at the surface. For high/low-flashing light regime, a periodic piece-wise constant irradiance (c.f. Figure 2) is applied at the reactor surface. Let us denote by $I_{\max}$ (resp. $I_{\min}$) the maximum (resp. minimum)

irradiance and by $\eta \in (0,1)$ the duty cycle. We can then define the average irradiance by

$$I_\eta := \eta I_{\max} + (1-\eta) I_{\min}. \tag{9}$$

The reactor is assumed to be illuminated continuously with irradiance I_η for the constant light regime, whereas in the high/low light regime, we assume that the reactor is exposed regularly between a high irradiance $I_{\max}$ for ηT and a low irradiance $I_{\min}$ for $(1-\eta)T$. See Figure 2.

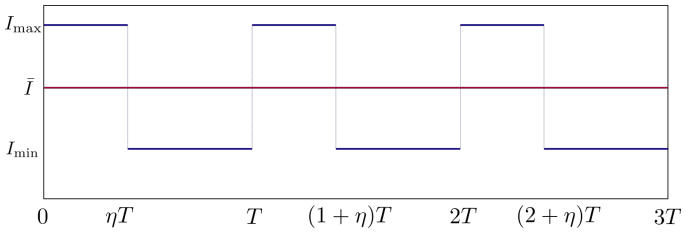

Fig. 2: Illustration of the two light regimes. The high/low regime (blue) in which the function I_s has a period T and switches from $I_{\max}$ to $I_{\min}$ for a time ηT and $(1-\eta)T$ respectively. The constant light regime (red) which is considered as the weighted average between $I_{\max}$ and $I_{\min}$.

Depending on the scale of T, we study two cases: when T is small compared with the Han model parameters τ, meaning that $T < \tau$ (the order of magnitude is milliseconds), we call this case *Small-T model* or high frequency model, and when T is large, *i.e.* when $T > 1/k_r$ (the order of magnitude is hours), we refer this case as *Large-T model* or low frequency model. The reduction methodology, depending on the light signal frequency, are now detailed.

2.2.2 Case I: Large-T model (low frequency model)

When light stays constant for a large enough time (we will justify later that large enough relies on the value of $1/k_r$), the dynamics of A reaches the steady state much faster than C (Hartmann et al, 2014). Then, it is possible to apply a fast-slow approximation by using the perturbation theory (Khalil, 2002). More precisely, we consider the slow manifold $A = \frac{1-C}{1+\tau\sigma I}$ (*i.e.* the pseudo steady state of A) to reduce the dynamics into one single equation on the photoinhibition state C:

$$\frac{\mathrm{d}C}{\mathrm{d}t} = -(\alpha(I) + k_r)C + \alpha(I), \tag{10}$$

with

$$\alpha(I) = \frac{k_d \tau (\sigma I)^2}{1+\tau\sigma I}. \tag{11}$$

System (7) has slow-fast timescales due to the factor k_d. For example, Table 1 presents some parameter values in the literature (Grenier et al, 2020;

Lamare et al, 2019), k_d is on the order of 10^{-4}. Then, the entries of the following matrices:

$$\begin{pmatrix} \sigma I + \frac{1}{\tau} & \frac{1}{\tau} \\ \sigma I & \frac{k_r}{k_d} + \sigma I \end{pmatrix} \quad \text{and} \quad \begin{pmatrix} \frac{1}{\tau} \\ \sigma I \end{pmatrix}$$

have values greater than 0.1 when considering an irradiance I in the order of $1000\,\mu\text{mol}\,\text{m}^{-2}\text{s}^{-1}$. The theory of slow/fast manifolds (Khalil, 2002) holds for autonomous systems. Although our system is nonautonomous, we can apply this principle to the system (7) in the interval $(0, \eta T)$ considering constant light equal to $I_{\max}$ and then considering the system with constant light $I_{\min}$ in the interval $(\eta T, T)$ since light do not affect the timescales of the system. The periodic solution of this system is computed in Appendix A.1.

2.2.3 Case II: Small-T model (high frequency model)

When light varies very rapidly compared to the system dynamics, the dynamics of the photoinhibition state C stays approximately constant (Hartmann et al, 2014). Under the assumption that C is constant, we can then apply averaging methods (Sanders et al, 2007) to simplify the system (7) into one equation on the open state A:

$$\frac{\mathrm{d}A}{\mathrm{d}t} = -\left(\sigma I + \frac{1}{\tau}\right) A + \frac{k_r - k_d \sigma \overline{IA}}{\tau(k_d \sigma \bar{I} + k_r)}, \tag{12}$$

with $\bar{I} = \frac{1}{T}\int_0^T I(t)\mathrm{d}t$ and $\overline{IA} = \frac{1}{T}\int_0^T I(t)A(t)\mathrm{d}t$. The details of this deduction and the solution of the system are described in Appendix A.2.

2.3 Accounting for the light gradient

Photobioreactors are illuminated at the surface and the light is attenuated along the depth z due to the light absorption and scattering. The generalized Beer-Lambert law is chosen for modelling this phenomenon:

$$I(y) \coloneqq I_s e^{-y}. \tag{13}$$

where $y := \varepsilon(X)z$, is the so-called local optical depth (Bernard and Lu, 2021). The vertical position is denoted by z. The light extinction coefficient $\varepsilon(X) > 0$ depends on the concentration of the microalgae X. Local optical depth (dimensionless) is a concept that integrates the attenuation of light due to pigment absorption and scattering. At local optical depth y, the light perceived is the fraction e^{-y} of the irradiance at the bioreactor surface. The advantage of this formulation is that it can integrate nonlinear effects of the extinction coefficient due to multiscattering (Morel, 1988). The darkest reactor part is characterized by a low remaining light, typically $\frac{I_{\text{out}}}{I_{\text{in}}} < 0.1$ which corresponds to the case $y > 2.3$ (Bernard et al, 2015). Some of our results hold for small values of local optical depth (meaning $y < 1$, where light extinction is lower than 36%).

Here, we assume that the algal biomass does not change at the considered timescale. From the definition of light attenuation (13), we denote by $I_H(y) = I_{\max}e^{-y}$ (resp. $I_L(y) = I_{\min}e^{-y}$) the high irradiance (resp. the low irradiance) at local optical depth y.

When illuminated by a constant irradiance I_η, the irradiance perceived at local optical depth y is given by $I_M(y) = I_\eta e^{-y}$. By choosing I_η as (9), we guarantee that the continuous light regime and the high/low flashing light regime provide the same amount of energy. Our objective is to compare the average growth rate for these two systems.

2.4 Model limitations

This model does not represent all the mechanisms involved in the photosynthesis, and how other factors such as temperature, pH or nutrients affect growth rate. It assumes that growth rate is driven by the PSII dynamics. For the considered timescales (from mseconds to hours), the dynamics of Calvin's cycle, and especially through RubisCo is not considered as a limiting factor. The pigment change as an acclimation mechanism to a varying light is also not represented. However, it has been shown that for fast varying light signal, cells acclimate to average irradiance (Combe et al, 2015), which is kept constant along our study.

2.5 Exact asymptotic solution of the Han model

For any initial condition of the Han model states (A and C), we prove in Lemma 2 that, for a periodic signal of light I, the solution of (7) converges to the unique periodic solution. This property is used to focus on the asymptotic periodic solution for the two models. We define the asymptotic exact T-averaged growth rate $\bar{\mu}^{\mathrm{T}}$ by

$$\bar{\mu}^{\mathrm{T}}(y) = \frac{1}{T}\int_0^T \mu(y,t)\mathrm{d}t, \tag{14}$$

where μ is defined in (3) and A is considered as the periodic solution of (1). Using the definition of M in (8), let us denote $M_H(y) = M(I_H(y))$, $N_H(y) = N_H(I_H(y))$, $M_L(y) = M(I_L(y))$, $N_L(y) = N(I_L(y))$.

Lemma 1 The system (7) under the periodic high/low light regime admits a unique periodic solution (A_p, C_p).

The computations of this periodic solution are given in Appendix A.3.

Lemma 2 All solutions of (7) under the periodic high/low light regime converge to the periodic solution.

Proof Let $(A, C)^T$ a solution of (7) under high/low light regime and $(A_p, C_p)^T$ the periodic solution of (7). Then $\xi := (A, C)^T - (A_p, C_p)^T$ is a solution of the impulsive differential equation

$$\begin{cases} \dot{\xi}(t) &= -M(t)\xi(t), \quad \text{for } t \neq t_k, \\ \xi(t_k^+) &= \xi(t_k), \end{cases}$$

where

$$t_0 = 0,$$
$$t_k = \begin{cases} t_{k-1} + \eta T, & \text{if } k \text{ is odd}, \\ t_{k-1} + (1-\eta)T, & \text{if } k \text{ is even}, \end{cases}$$

is the sequence of discontinuities of the light function in the high/low regime and M is defined in (8). Let us denote by Λ_H, Λ_L the largest eigenvalues of the matrices M_H and M_L respectively. Note that $t_{2k} = kT$. Our goal is to prove that for every $k \in \mathbb{N}$ we have

$$\|\xi(t)\| \leq e^{-k\Lambda_\eta T}\|\xi(0)\|\,, \quad \forall t \in [t_{2k}, t_{2(k+1)}], \tag{15}$$

where $\Lambda_\eta = \eta\Lambda_H + (1-\eta)\Lambda_L$. Since the matrix is constant in the intervals (t_k, t_{k+1}) for every k, we have that

$$\xi(t) = \begin{cases} e^{-tM_H}\xi(0), & \text{if } t \in [t_0, t_1), \\ e^{-tM_L}e^{-\eta T M_H}\xi(0), & \text{if } t \in [t_1, t_2]. \end{cases}$$

This implies that

$$\|\xi(t)\| = \begin{cases} \|e^{-tM_H}\|\|\xi(0)\|, & \text{if } t \in [t_0, t_1), \\ \|e^{-tM_L}e^{-\eta T M_H}\|\|\xi(0)\|, & \text{if } t \in [t_1, t_2], \end{cases}$$

and $\|\xi(t)\| \leq \|\xi(0)\|$ for $t \in [t_0, t_2]$. Now, suppose that (15) holds for k, let us prove that this also holds for $k+1$. Let $t \in [t_{2(k+1)}, t_{2(k+2)}]$, then

$$\xi(t) = \begin{cases} e^{-tM_H}\xi(t_{2(k+1)}) & \text{if } t \in [t_{2(k+1)}, t_{2(k+1)+1}), \\ e^{-tM_L}e^{-\eta T M_H}\xi(t_{2(k+1)}) & \text{if } t \in [t_{2(k+1)+1}, t_{2(k+2)}]. \end{cases}$$

As $\xi(t_{2(k+1)}) = e^{-(1-\eta)TM_L}e^{-\eta T M_H}\xi(t_{2k})$, and $\|\xi(t_{2k})\| \leq e^{-k\Lambda_\eta T}\|\xi(0)\|$, then

$$\begin{aligned} \|\xi(t_{2(k+1)})\| &= \|e^{-(1-\eta)TM_L}e^{-\eta T M_H}\xi(t_{2k})\| \\ &\leq e^{-T\Lambda_\eta}\|\xi(t_{2k})\| \\ &\leq e^{-(k+1)T\Lambda_\eta}\|\xi(0)\|, \end{aligned}$$

and we can conclude that

$$\begin{aligned} \|\xi(t)\| &= \begin{cases} \|e^{-tM_H}\|e^{-(k+1)T\Lambda_\eta}\|\xi(0)\| & \text{if } t \in [t_{2(k+1)}, t_{2(k+1)+1}), \\ \|e^{-tM_L}e^{-\eta T M_H}e^{-(k+1)T\Lambda_\eta}\|\xi(0)\| & \text{if } t \in [t_{2(k+1)+1}, t_{2(k+2)}). \end{cases} \\ &\leq e^{-(k+1)T\Lambda_\eta}\|\xi(0)\|. \end{aligned}$$

Finally, as (15) holds, taking $k \to \infty$ we conclude that $\|\xi(t)\| \to 0$ as $t \to \infty$. □

Solving (7) in periodic case and using the definition of the growth rate (3), it is possible to analytically compute the exact T-average growth rate in the high/low-flashing light as

$$\bar{\mu}^{\mathrm{T}}(y) = \eta\mu_S(I_H(y)) + (1-\eta)\mu_S(I_L(y)) - \frac{K\sigma}{T}\delta(y,T), \tag{16}$$

where the function μ_S is defined in (4), δ is the first component of the vector

$$\begin{aligned}\Delta = \Big[& I_H(y)M_H^{-1}(y)\left(\mathrm{Id} - e^{-\eta T M_H(y)}\right)\left(\mathrm{Id} - e^{-(1-\eta)TM_L(y)}e^{-\eta T M_H(y)}\right)^{-1}\left(\mathrm{Id} - e^{-(1-\eta)TM_L(y}\right) \\ & - I_L(y)M_L^{-1}(y)\left(\mathrm{Id} - e^{-(1-\eta)TM_L(y}\right)\left(\mathrm{Id} - e^{-\eta T M_H(y)}e^{-(1-\eta)TM_L(y)}\right)^{-1}\left(\mathrm{Id} - e^{-\eta T M_H(y)}\right)\Big] \\ & \cdot \left(M_H^{-1}(y)N_H(y) - M_L^{-1}(y)N_L(y)\right),\end{aligned} \tag{17}$$

with Id the identity matrix in $\mathbb{R}^{2\times 2}$. The details of the computations are given in A.4.

3 Study of Case I: Slowly varying irradiance

In this section, we present an analysis based on the growth rate calculated using the large-T model. We show in particular that the average growth rate can be greater than the values of the PI-curve derived from the Han model. We give the conditions to get an enhanced average growth rate based on the local convexity of the function μ_S.

3.1 Average growth rate and analysis

In large-T model, the growth rate can be derived from (3) as

$$\mu = K\sigma IA = (1-C)\gamma(I), \tag{18}$$

with $\gamma(I) = \frac{K\sigma I}{1+\tau\sigma I}$ and C the periodic solution of (10). For a given local optical depth y, the T-average growth rate for the high/low light regime can be computed explicitly by

$$\bar{\mu}^{\mathrm{T}}(y) = \frac{1}{T}\int_0^T \mu(y,t)\mathrm{d}t = \eta\mu_S(I_H(y)) + (1-\eta)\mu_S(I_L(y)) + \frac{\zeta_1(y,\eta,T)\zeta_2(y)}{Tk_r}, \tag{19}$$

with

$$\begin{aligned}\zeta_1(y,\eta,T) &= \frac{\left(1 - e^{-(\alpha_L(y)+k_r)T(1-\eta)}\right)\left(1 - e^{-(\alpha_H(y)+k_r)T\eta}\right)}{1 - e^{-(\alpha_L(y)+k_r)T(1-\eta)-(\alpha_H(y)+k_r)T\eta)}}, \\ \zeta_2(y) &= \left(\frac{\alpha_H(y)}{\alpha_H(y)+k_r} - \frac{\alpha_L(y)}{\alpha_L(y)+k_r}\right)\left(\mu_S(I_H(y)) - \mu_S(I_L(y))\right),\end{aligned}$$

where α is defined in (11) and we extend the notation as $\alpha_H(y) := \alpha(I_H(y))$ and $\alpha_L(y) := \alpha(I_L(y))$. The details of the computations are presented in A.1. Let us denote by $\mu_S^\eta(y)$ the convex combination in (19):

$$\mu_S^\eta(y) := \eta\mu_S(I_H(y)) + (1-\eta)\mu_S(I_L(y)). \tag{20}$$

When T is large enough, we can approximate the T-average growth rate by (20). Indeed, it is straightforward to see that $0 \leq \zeta_1(y,\eta,T) \leq 1$ and $0 \leq \frac{\alpha(I)}{\alpha(I)+k_r} \leq 1$, therefore, one has

$$\left|\bar{\mu}^{\mathrm{T}}(y) - \mu_S^{\eta}(y)\right| = \left|\frac{\zeta_1(y,\eta,T)\zeta_2(y)}{Tk_r}\right| \leq \frac{|\mu_S(I_H(y)) - \mu_S(I_L(y))|}{Tk_r} \leq \frac{\mu_{\max}}{Tk_r},$$

where the last inequality is obtained by taking the maximum growth rate of the Han model given by (5). This leads to the following result.

Theorem 1 *For a large enough period T, for every local optical depth $y \geq 0$ we have $\lim_{T\to+\infty} \bar{\mu}^{T}(y) = \mu_S^{\eta}(y)$. Furthermore, the convergence is uniformly in y and $\left|\bar{\mu}^{T}(y) - \mu_S^{\eta}(y)\right| = \mathcal{O}(1/T)$.*

3.2 Enhancement of the growth rate

Growth rate in high/low light regime can be enhanced or reduced compared to that of the constant light regime. More precisely, this relies on the local convexity of the function μ_S with respect to the irradiance I. Depending on the value of I, this can be either convex or concave. The next lemma clarifies the critical value of the irradiance.

Lemma 3 There exists an irradiance I_c, for which μ_S is a strictly convex function in $(I_c, +\infty)$ and strictly concave in $(0, I_c)$. This value only depends on the parameters (k_d, k_r, τ, σ), *i.e.*,

$$I_c = \begin{cases} \frac{2}{\sigma\sqrt{\frac{k_d}{k_r}}\tau} \cos\left(\frac{1}{3}\arccos\left(\frac{\sqrt{\tau}}{2\sqrt{\frac{k_d}{k_r}}}\right)\right) & \text{if } \tau \leq 4\frac{k_d}{k_r}, \\ \frac{2}{\sigma\sqrt{\frac{k_d}{k_r}}\tau} \cosh\left(\frac{1}{3}\operatorname{arccosh}\left(\frac{\sqrt{\tau}}{2\sqrt{\frac{k_d}{k_r}}}\right)\right) & \text{if } \tau > 4\frac{k_d}{k_r}. \end{cases} \tag{21}$$

The proof is given in B. This lemma enables us to state the next theorem, which is our main result. In this theorem, we provide conditions to enhance the growth rate, meaning that the average growth rate calculated in (19) is greater than the growth rate obtained for the continuous light regime I_η. Also, Figure 5a illustrates in the curve μ_S the value of I_c positioned on the right of I_{opt}.

Theorem 2 *Let I_c defined by (21). For every couple (I_{max}, I_{min}), such that $I_{max} > I_{min} > I_c$, there exists $T > 0$ and $\eta \in (0,1)$ such that*

$$\bar{\mu}^{T}(0) \geq \mu_S(I_\eta), \tag{22}$$

where $I_\eta = \eta I_{max} + (1-\eta) I_{min}$.

Proof Setting $y = 0$ in (19) gives

$$\bar{\mu}^{\mathrm{T}}(0) = \eta\mu_S(I_{\max}) + (1-\eta)\mu_S(I_{\min}) + \frac{\zeta_1(0,\eta,T)\zeta_2(0)}{Tk_r}.$$

Recall that

$$\begin{aligned}\zeta_2(0) &= \Big(\frac{\alpha_H(0)}{\alpha_H(0)+k_r} - \frac{\alpha_L(0)}{\alpha_L(0)+k_r}\Big)\big(\mu_S(I_H(0)) - \mu_S(I_L(0))\big),\\ &= \Big(\frac{\alpha(I_{\max})}{\alpha(I_{\max})+k_r} - \frac{\alpha(I_{\min})}{\alpha(I_{\min})+k_r}\Big)\big(\mu_S(I_{\max}) - \mu_S(I_{\min})\big).\end{aligned}$$

In $(I_c, +\infty)$ the function μ_S is decreasing, then $\mu_S(I_{\max}) - \mu_S(I_{\min}) < 0$. Moreover, the function $I \mapsto \frac{\alpha(I)}{\alpha(I)+k_r}$ is increasing, hence $\zeta_2(0) < 0$. On the other hand, one has $0 \le \zeta_1(0,\eta,T) \le 1$ and $0 \le \frac{\alpha(I)}{\alpha(I)+k_r} \le 1$ for $I \ge 0$. All together implies that

$$\bar{\mu}^{\mathrm{T}}(0) \ge \eta\mu_S(I_{\max}) + (1-\eta)\mu_S(I_{\min}) + \frac{1}{Tk_r}\left(\mu_S(I_{\max}) - \mu_S(I_{\min})\right). \tag{23}$$

To conclude, we have to find T such that the right-hand side of (23) is greater than $\mu_S(I_\eta)$ which is equivalent to the condition

$$\frac{1}{Tk_r} \le \frac{\mu_S(I_\eta) - \eta\mu_S(I_{\max}) - (1-\eta)\mu_S(I_{\min})}{\mu_S(I_{\max}) - \mu_S(I_{\min})}. \tag{24}$$

Since $\mu_S(I)$ is convex and decreasing on interval $(I_c, +\infty)$, the right-hand side of (24) is always positive. Therefore, a couple (T,η) verifying condition (24) will ensure the inequality (22). This concludes the proof. □

For $I_{\max}, I_{\min} \in (I_c, +\infty)$ and $y = 0$ (*i.e.*, at the surface), one can find a period T and a duty cycle η such that the T-average growth rate under the high/low light regime is greater than the constant average light regime. Based on the condition (24), if η is near to 0 or 1 we need larger T, since the right-hand side of the inequality approaches to zero in this case. This improvement can also be valid for other choices of light (see Figure 5).

On the other hand, one can see that a condition between T and η is needed to give an interpretation of this improvement in the growth rate. Assume that the condition (24) holds for some T and η. Since $\mu_S(I_\eta) \ge \mu_S(I_{\max})$, then one has

$$\begin{aligned}\frac{1}{Tk_r} &\le \frac{\mu_S(I_\eta) - \eta\mu_S(I_{\max}) - (1-\eta)\mu_S(I_{\min})}{\mu_S(I_{\max}) - \mu_S(I_{\min})}\\ &\le \frac{\mu_S(I_{\max}) - \eta\mu_S(I_{\max}) - (1-\eta)\mu_S(I_{\min})}{\mu_S(I_{\max}) - \mu_S(I_{\min})}\\ &= 1-\eta,\end{aligned}$$

or, in other words, $(1-\eta)T \ge \frac{1}{k_r}$. The time needed for recovering a damaged reaction center is $\frac{1}{k_r}$ and, $(1-\eta)T$ represents the time that the system is exposed under the low light. Therefore, by considering the exposed time under the low light which is larger than recovering time $\frac{1}{k_r}$, the average growth rate

at the surface can be enhanced in the high/low light regime. Assuming T large enough, we have the approximation

$$\bar{\mu}^{\mathrm{T}}(y) \approx \mu_S^{\eta}(y). \tag{25}$$

Then we can state the next theorem which will provide the optimal duty cycle η for enhancing the growth rate.

Theorem 3 *For large T, choosing $I_{max} > I_{\min} > I_c$, at the top of the bioreactor, there exists $\eta \in (0,1)$ which maximize the difference between the average growth rate in the high/low-flashing light regime, leading to a T-average growth rate larger than the one in continuous light regime.*

Proof Setting $y = 0$. In the limit case of the large-T model, we approximate the average growth rate with (25). The optimum η_{opt} is defined as

$$\eta_{\mathrm{opt}} := \underset{\eta\in(0,1)}{\operatorname{argmax}}\, \eta\mu_S(I_{\max}) + (1-\eta)\mu_S(I_{\min}) - \mu_S(I_\eta),$$

which solution is such that

$$\frac{\mathrm{d}}{\mathrm{d}I}\mu_S(I_{\eta_{\mathrm{opt}}}) = \frac{\mu_S(I_{\max}) - \mu_S(I_{\min})}{I_{\max} - I_{\min}}, \tag{26}$$

and the existence is ensured by the mean value theorem. □

This optimal η is actually the one which is capable of achieving the maximal difference between $\bar{\mu}^{\mathrm{T}}(0)$ and $\mu_S(I_\eta)$. Moreover, (26) can be rewritten as

$$0 = \left[1 + \tau\sigma I_{\eta_{\mathrm{opt}}} + \frac{k_d}{k_r}\tau(\sigma I_{\eta_{\mathrm{opt}}})^2\right]^2 \frac{\mu_S(I_{\max}) - \mu_S(I_{\min})}{K\sigma(I_{\max} - I_{\min})} + \frac{k_d}{k_r}\tau(\sigma I_{\eta_{\mathrm{opt}}})^2 - 1.$$

4 Study of Case II: fast varying light

In this section, we present the value of the T-average growth rate using the Small-T model, meaning that $T < \tau$. Recall that τ is the time during which one photon is processed in the PSU, thus T is in the order of milliseconds. We prove that the average growth rate, in the limit, corresponds to $\mu_S(I_\eta)$, then we provide an analysis in the flashing light regime, and we define the optimal local optical depth in this case.

4.1 Average growth rate

Recall that, by definition (14), the T-average growth rate can be computed by $\bar{\mu}^{\mathrm{T}} = \frac{1}{T}\int_0^T K\sigma I A \mathrm{d}t = K\sigma\overline{IA}$. Then $\bar{\mu}^{\mathrm{T}}$ is computed by

$$\bar{\mu}^{\mathrm{T}}(y) = \frac{K\sigma k_r I_M(y)\big(1 + \xi_1(y)\xi_2(y,T)\big)}{k_r + k_r\tau\sigma I_M(y) + k_d\tau\big(\sigma I_M(y)\big)^2 + k_d\sigma I_M(y)\xi_1(y)\xi_2(y,T)}, \tag{27}$$

where

$$\xi_1(y) = \frac{\sigma\big(I_H(y) - I_L(y)\big)^2 \eta(1-\eta)}{\tau \beta_H(y)\beta_L(y)},$$
$$\xi_2(y,T) = \frac{(1-e^{-\beta_H(y)\eta T})(1-e^{-\beta_L(y)(1-\eta)T})}{T(1-e^{-\beta_H(y)\eta T-\beta_L(y)(1-\eta)T})} \frac{\eta\beta_H(y)+(1-\eta)\beta_L(y)}{\eta(1-\eta)\beta_H(y)\beta_L(y)} - 1,$$

$\beta_H(y) := \beta(I_H(y))$ and $\beta_L(y) := \beta(I_L(y))$. The details of the computation are given in A.2. Since

$$\lim_{T\to 0} \frac{(1-e^{-\beta_H(y)\eta T})(1-e^{-\beta_L(y)(1-\eta)T})}{T(1-e^{-\beta_H(y)\eta T-\beta_L(y)(1-\eta)T})} = \frac{\eta(1-\eta)\beta_H(y)\beta_L(y)}{\beta_H(y)+\beta_L(y)},$$

one has $\lim_{T\to 0} \xi_2(y,T) = 0$. This leads to the following result.

Theorem 4 *For rapid light alternation, one has for every local optical depth* $y > 0$ $\lim_{T\to 0} \bar{\mu}^T(y) = \mu_S(I_M(y))$.

In the limit, when $T \to 0$, the growth rate of the high/low-flashing light is the same as the growth rate at steady state of A (full light integration) by considering the irradiance I_η. In this case, the algae perceives the average irradiance for growing and there is no possible gain in growth rate compared to continuous light.

4.2 Small-T flashing light

Flashing light corresponds to the particular case of the high/low-flashing light when $I_{\min} = 0$. Based on our previous analysis, we present the local optical depth at which the algae culture perceives the optimal irradiance for growing.

Assume that the approximation $\bar{\mu}^{\mathrm{T}}(y) \approx \mu_S(I_\eta(y))$ holds. By Theorem 4, the light perceived by the algae at local optical depth y is $I_\eta(y) = \eta I_{\max} e^{-y}$. In this case, we can give an explicit expression for the local optical depth at which the algae culture perceives the optimal light, and consequently, the depth where the optimal light is perceived. This expression depends on the duty cycle η which, in practice, can be settled and then, we can select the local optical depth in a certain range of values. We define the *optimal local optical depth* as the local optical depth in which the average growth rate achieves the maximum of the growth rate.

Lemma 4 Considering flashing light, let $I_{\max}$ the maximum irradiance provided at the top of the bioreactor, η the duty cycle and σ, k_d, k_r, τ the parameters of the Han model. The optimal local optical depth is given by

$$y_{\mathrm{opt}} = \ln\left(I_{\max}\sigma\sqrt{\frac{k_d}{k_r}\tau\eta}\right) \tag{28}$$

Proof The growth rate, considering flashing light and the limit case of the small-T model correspond to

$$\bar{\mu}^{\mathrm{T}}(y) = \mu_S(\eta I_{\max} e^{-y}) = \mu_S(I_{\max} e^{-(y-\ln(\eta))}).$$

Matching the value of the optimal light of the function μ_S given by (6) and the growth rate calculated above, we obtain the equality

$$I_{\max} e^{-(y_{\mathrm{opt}} - \ln \eta)} = \frac{1}{\sigma\sqrt{\frac{k_d}{k_r}\tau}},$$

and isolating y_{opt} we get the value (28). □

As η tends to zero, y_{opt} can take negative values. Negative values are meaningless, the algae culture does not perceive the optimal light in this case and all the culture is under the photo-limited condition. Hence, the choice of the duty cycle η impacts productivity. For including the optimal light into the culture, we have to consider the inequality

$$\eta \geq \frac{1}{I_{\max}\sigma\sqrt{\frac{k_d}{k_r}\tau}}.$$

Using the definition of I_{opt}, this is equivalent to the condition:

$$\eta \geq \frac{I_{\mathrm{opt}}}{I_{\max}}.$$

In conclusion, for every value of η in the range of $[I_{\mathrm{opt}}/I_{\max}, 1)$ the optimal light is perceived in the culture. By setting $\eta = I_{\mathrm{opt}}/I_{\max}$, the optimal light is then perceived at the top of the culture.

Considering $y = aXz$ where, X is the concentration of the culture, z is the depth and a is the light attenuation constant. Then, the depth at which the culture perceives the optimal light intensity is given by

$$z_{\mathrm{opt}} = \frac{1}{aX} \ln\left(I_{\max}\sigma\sqrt{\frac{k_d}{k_r}\tau\eta}\right).$$

So, as the concentration increase through time, z_{opt} decrease. One way to counteract this effect is to increase the value of the duty cycle η.

5 Study of Case III: the intermediate case

We analyzed the large and the small-T model, then gave the limit of the T-averaged growth rate in Theorem 1 and Theorem 4 when $T \to +\infty$ and $T \to 0$ respectively. Meanwhile, we evaluated the T-average growth rate without considering the simplified models given in (16) named as the asymptotic exact growth rate. In this section, we show that the limits of (16) are the same as the results in Theorem 1 and Theorem 4.

Proposition 5 *The exact average growth rate* (16) *converges to* μ_S^η *as* $T \to +\infty$ *and it also converges to* $\mu_S(I_M)$ *when* $T \to 0$.

Proof Let us first prove that if $T \to +\infty$, then $\bar{\mu}^{\mathrm{T}}$ given by (16) converges to μ_S^η. The eigenvalues of the matrices M_H and M_L are positive (see Appendix A.5) and then, the exponential matrices

$$e^{-\eta T M_H(y)} \quad \text{and} \quad e^{-(1-\eta)TM_L(y)}$$

converge to the zero matrix as $T \to +\infty$ for every local optical depth y. Thus,

$$\lim_{T\to+\infty} \Delta = \left[I_H(y)M_H^{-1}(y) - I_L(y)M_L^{-1}(y)\right]\left(M_H^{-1}(y)N_H(y) - M_L^{-1}(y)N_L(y)\right),$$

where Δ is defined in (17). From the exact growth rate given by (16), we can also conclude that

$$\lim_{T\to+\infty} \bar{\mu}^{\mathrm{T}}(y) = \eta\mu_s(I_H(y)) + (1-\eta)\mu_S(I_L(y)) = \mu_S^\eta(y),$$

which is the result of Theorem 1. Now, for the other case, we have that

$$\lim_{T\to 0} \frac{\Delta}{T} = \eta(1-\eta)M_\eta^{-1}(y)(I_H(y)M_L(y) - I_L M_H(y))[(M_H^{-1}(y)N_H(y) - M_L^{-1}(y)N_L(y)],$$

where $M_\eta(y) = \eta M_H(y) + (1-\eta)M_L(y)$. We can manipulate this term and get that

$$\begin{aligned}\lim_{T\to 0} \frac{\Delta}{T} &= M_\eta^{-1}\left[-I_\eta N_\eta + \eta I_H M_\eta M_H^{-1} N_H + (1-\eta) I_L M_\eta M_L^{-1} N_L\right](y) \\ &= -I_\eta(y)M_\eta^{-1}(y)N_\eta(y) + \eta I_H(y)M_H^{-1}(y)N_H(y) + (1-\eta)I_L(y)M_L^{-1}(y)N_L(y).\end{aligned}$$

Replacing this limit in (16), we conclude that

$$\lim_{T\to 0} \bar{\mu}^{\mathrm{T}}(y) = \mu_S(I_\eta(y)).$$

This corroborates the behavior of the mean of the growth rate in the large-T and small-T models. □

6 Illustration with simulation studies

6.1 Parameter settings

The Han model parameters in literature are different depending on the authors and the studied species. Here we consider the values taken from three studies (Grenier et al, 2020; Lamare et al, 2019) and present in Table 1.

In this section, we provide some numerical tests to illustrate the two approximations and the exact solution of the Han system.

6.2 Quality of the approximated solution

First, we illustrate the difference between the two approximations and the exact solution. In Figure 3 the solution of A and C is plotted for $T = 0.5\,\mathrm{s}$ and $T = 3600\,\mathrm{s}$. For the small-T model, 0.5 s is considered. The large-T model is then a non-accurate approximation. As for $T = 3600\,\mathrm{s}$ we need to drop the assumption of C constant. In this case, the small-T model is far from the real

Parameter	Symbol	(Grenier et al, 2020)	(Lamare et al, 2019)	Unit
Recovery rate	k_r	$6.8 \cdot 10^{-3}$	$4.8 \cdot 10^{-4}$	s^{-1}
Damage rate	k_d	$2.99 \cdot 10^{-4}$	$2.99 \cdot 10^{-4}$	-
Turnover time	τ	0.25	6.8493	s
Effective cross-section	σ	0.047	0.0029	$m^2\,\mu mol^{-1}$
Growth rate coefficient	K	$8.7 \cdot 10^{-6}$	$3.6467 \cdot 10^{-4}$	-
Optimal light	I_{opt}	202.93	166.94	$\mu mol\,m^{-2}s^{-1}$
Critical light	I_c	414.29	356.24	$\mu mol\,m^{-2}s^{-1}$

Table 1: Parameter values for Han Model.

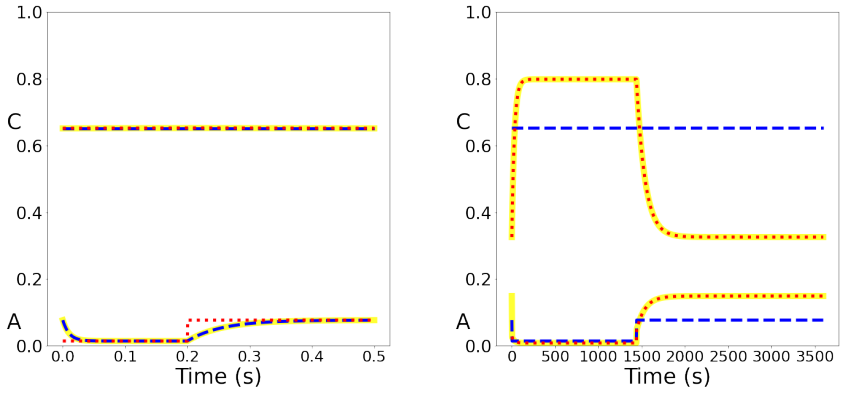

(a) $T = 0.5$s (b) $T = 3600$s

Fig. 3: Comparison of the two modelling approximations with the exact solution of the states of the Han model. The state A and C of the exact solutions (7) (continuous yellow line), of the small-T model (12) (segmented blue line) and of the large-T model (10) (segmented red line) are provided for $I_{max} = 2000\,\mu mol\,m^{-2}\,s^{-1}$, $I_{min} = 300\,\mu mol\,m^{-2}\,s^{-1}$, $\eta = 0.4$, $y = 0$ and four different values of T.

solution. We observe that A and C change between two values, these values correspond to the steady states considering I_{max} and I_{min}.

As expected, one can see that (12) provides a good approximation for small period (in this case for $T = 0.5\,s$) and (10) provides a good approximation for large period ($T = 3600\,s$). On the other hand, the quality of the approximation depends on the time period T.

6.3 Connection between Case I and Case II

Here we study the connection of the average growth rate between the one obtained from the large-T model (10), the small-T model (12) and the exact model (7). More precisely, we compute the T-average growth rate at the surface $\bar{\mu}^{\mathrm{T}}(0)$ by varying the period T from $T = 0.01\,\mathrm{s}$ to $T = 36\,000\,\mathrm{s}$, and the results are shown in Figure 4a. As $T \to 0$ the average growth rate converges to the value $\mu_S(I_\eta(0)$, whereas $\bar{\mu}^{\mathrm{T}} \to \mu_\eta(0)$ when $T \to +\infty$. Moreover, the inequality (22) holds for $T >= 174\,\mathrm{s}$ as shown in Figure 4a, which is not the case in Figure 4b. Note that the time needed to process a photon (τ) and the time needed to recover a reaction center ($1/k_r$) are also given in Figure 4.

Small Period For $T \in (0, \tau]$ Small-T model gives a good approximation. As the light change in a timescale lower than the time of processing photons, in this case, the algae perceives the average of the light (i.e, I_η at the top).
Transition Period For $T \in (\tau, \frac{1}{k_r})$ the small period started to fail, and consider the large-T model is more accurate.
Large Period For $T \in [\frac{1}{k_r}, \infty)$ Large-T model fits. If a high light is combined with a low light, then some damaged reaction centers can be recovered, and we can get an improvement of the T-average growth rate compared to the continuous light regime.

6.4 Improvement of the growth rate

As shown in Theorem 2, there exists an improvement in the growth rate when the irradiance I_H and I_L are greater than the value of I_c as the case presented in Figure 5a. Unfortunately, the irradiance decreases when the local optical depth increases breaking the condition $I_H, I_L \geq I_c$, and then, the improvement is no longer perceived. In Figure 5d, the T-average growth rate (black curve) is plotted as a function of the local optical depth, and it has greater values than the PI-curve of the Han model (blue curve). This means that the improvement perceived at the surface are still true when going deeper in the culture, but for larger values of y the T-average growth rate is smaller than the blue curve. Roughly speaking, this improvement is perceived in the section of the bioreactor receiving strong irradiance that inhibits photosynthesis.

It is possible to relax the condition $I_{\max} > I_{\min} > I_c$ in Theorem 2. For example, let us fix $I_{\max} > I_c$ and $I_{\min} < I_c$ as is shown in Figure 5b, for the two different values of the duty cycle η_1 and η_2, the average growth rate is denoted $\mu_S^{\eta_1}$ and $\mu_S^{\eta_2}$ respectively. In this case, the average growth rate considering the duty cycle η_2 is greater than the growth rate in continuous light with the same average light $\mu_S(I_{\eta_2})$, but for the duty cycle η_1 the growth rate is lower than with the continuous light. If we consider, for example, the parameters of Grenier et al (2020) where $I_c = 202.93$ ($\mu\mathrm{mol\,m^{-2}s^{-1}}$) (see Table 1), $I_{\max} = 2000$ ($\mu\mathrm{mol\,m^{-2}s^{-1}}$), $I_{\min} = 100$ ($\mu\mathrm{mol\,m^{-2}s^{-1}}$). For η_1 the growth rate in continuous light regime is 13.7% larger than the average growth rate, and, for η_2 it is 12.5% smaller.

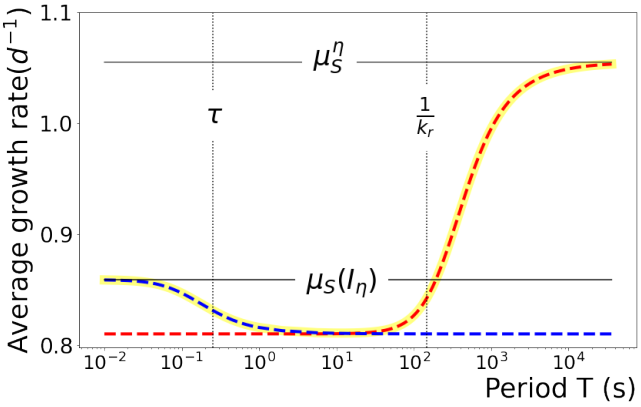

(a) $I_{\max} = 2000\,\mu\text{mol}\,\text{m}^{-2}\text{s}^{-1}$ and $I_{\min} = 10\,\mu\text{mol}\,\text{m}^{-2}\text{s}^{-1}$.

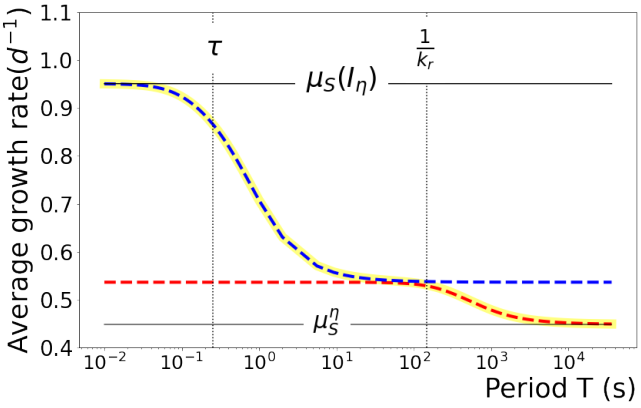

(b) $I_{\max} = 2000\,\mu\text{mol}\,\text{m}^{-2}\text{s}^{-1}$ and $I_{\min} = 10\,\mu\text{mol}\,\text{m}^{-2}\text{s}^{-1}$.

Fig. 4: The exact average growth rate (16) (continuous yellow line), the average growth rate of the large-T model (19) (segmented red line) and the average growth rate of the small-T model (27) (segmented blue line). The period T is plotted in log scale. In this case $\eta = 0.5$

On the other hand, some selections for $I_{\min}$ can only give lower values of the T-average growth rate comparing with the PI-curve as we can see in Figure 5c. In this case, every selection of η provides a T-average growth rate lower than the PI-curve.

Figure 6 summarizes the behavior of the two models representing the simplifications of Case I and Case II. The exact growth rate is plotted in the form of a polygon. We can see that, for greater values of T, the exact growth rate coincides with the T-averaged growth rate of the large-T model. In this case,

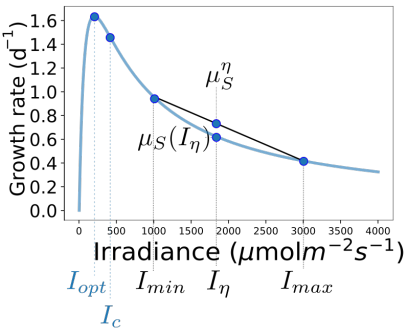

(a) Diagram of the Theorem 2 in which $I_{\max}$ and $I_{\min}$ are greater than I_c. In this configuration, for each $\eta \in (0.1)$ we can find T for which $\mu_S(I_\eta) > \mu_S(I_\eta)$.

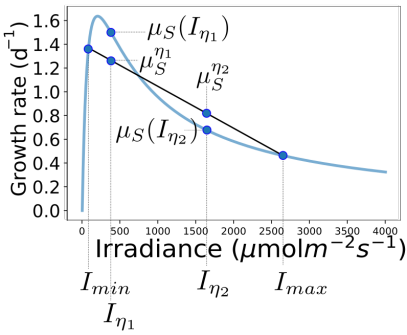

(b) When $I_{\min} < I_c$, we can still improve the average growth rate for some values of η. In this case, $\mu_S^{\eta_1} > \mu_S(I_{\eta_2})$ and $\mu_S^{\eta_2} < \mu_S(I_{\eta_1})$ for η_1.

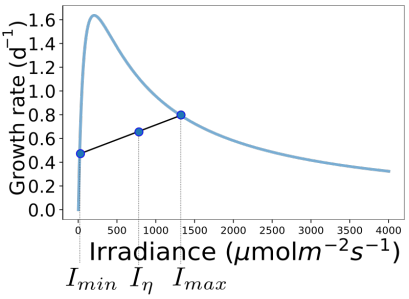

(c) For some configurations, it is impossible to find a fraction η and a period T for which $\mu_S^\eta > \mu_S(I_\eta)$.

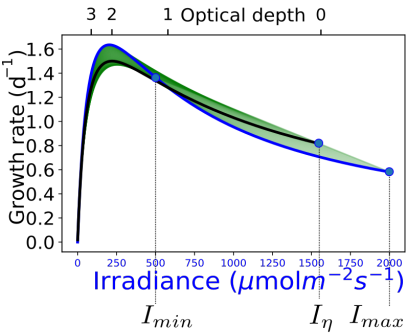

(d) The green area represents all the possible values for μ_S^η if we vary the local optical depth and η for a given $I_{\max}$ and $I_{\min}$. The black line correspond to the values of μ_S^η for a fixed value of η.

Fig. 5: Illustration of Theorem 2, where approximation $\bar{\mu}_S^T \approx \mu_S^\eta$ holds for different combinations of $I_{\max}, I_{\min}$ and η.

the hypotheses of Theorem 2 are satisfied. The red polygon corresponds to the surface of the bioreactor ($y = 0$) where the curve of the T-average growth rate of the large-T model is greater to the T-average growth rate of the small-T model due to Theorem 2. Note that in the small-T model, the average growth rate matches $\mu_S(I_\eta)$, which corresponds to the continuous light regime with the same average irradiance. As y becomes larger, the growth rate for Case I is lower than for the constant light regime, as shown in the green and blue polygon.

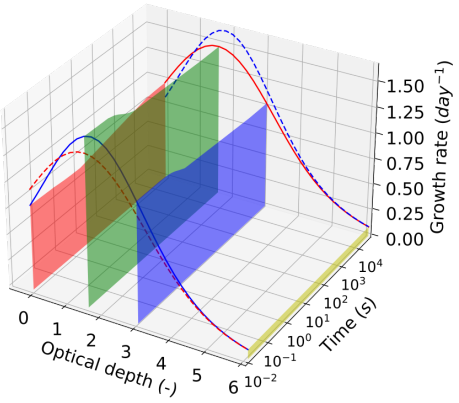

Fig. 6: Average growth rate as a function of period T for four different local optical depths. We set $I_{\max} = 2000\,\mu\text{mol}\,\text{m}^{-2}\,\text{s}^{-1}$, $I_{\min} = 500\,\mu\text{mol}\,\text{m}^{-2}\,\text{s}^{-1}$, $\eta = 0.5$. Average growth rate in the case II for small-T model (blue curve) and in the Case I for large-T model (red curve). For small values of the time we plotted in the continuous line the small-T model and analogous for the larger values of T.

7 Perspectives

Most of our computations are still valid if the acclimation is modelled as a variation of the cross-section σ as a fixed parameter, for example, in the model of (Nikolaou et al, 2016), σ is a function of the chlorophyll content, consequently, the value of A varies depending on the light at which the microalgae is acclimated. Then, in order to adapt our calculations, the parameter σ must change and be fixed in advance. Finally, two different light regimes can be compared changing the value of σ. On the other hand, Microalgae are subjected to stochastic changes in the light regime that they perceive due to the mixing of the bioreactor. Although, we do not consider mixing in the computations, our calculations could be extended if a simplification of the hydrodynamic is considered. For example, a continuously illuminated bioreactor could be divided in two sections: a thin layer close to the illuminated surface and another layer photolimited. Both layers would be associated with a characteristic light intensity, then, assuming we know the fraction of time that the algae spend in each layer, the computations of the average growth rate can be used. This approach was already considered with a similar model in Wu and Merchuk (2001), but considering that the irradiance in the photolimited layer is zero.

8 Conclusions

We analyze the T-averaged growth rate in the high/low flashing light configuration in two simplified cases: for large period T and small period T. In the

small-T model, we can simply approximate the T-average growth rate by considering $\mu_S(\eta I_H + (1-\eta)I_L)$, and for the large period T, we can approximate the T-average growth rate by considering $\eta\mu_S(I_H) + (1-\eta)\mu_S(I_L)$. In terms of growth rate, there is no distinction between the constant regime with light I_η and switching the light quickly between I_H and I_L in the time ηT and $(1-\eta)T$ respectively. In contrast, in the large-T model, we can improve the growth rate if we consider a low local optical depth. In this case, combining a high inhibiting irradiance and a lower irradiance with a period greater than $1/k_r$ (in the range of hours) in average, the growth rate will be higher than the one considering continuous light regime with the same average irradiance. Although, for higher local optical depth, the growth rate is lower than the constant light regime.

Acknowledgments. This project has received funding from the Digitalgaesation project within the European Union's Horizon 2020 research and innovation program under the Marie Skłodowska-Curie grant agreement No. 955520

Appendix A Analytical Computations

A.1 Case I: Large period T

For large period case, the evolution system (7) can be approximated by (10) which can be solved explicitly for a constant irradiance I as

$$C(y,t) = \frac{\alpha(I(y))}{\alpha(I(y))+k_r}(1-e^{-(\alpha(I(y))+k_r)t}) + e^{-(\alpha(I(y))+k_r)t}C(y,0), \quad t \in (0,T).$$

Moreover, the system is assumed to be periodic (*i.e.* $C(y,0) = C(y,T)$). For the constant light regime $I_M(y)$, one has $C(y,t) = \frac{\alpha(I_M(y))}{\alpha(I_M(y))+k_r}$, $\forall t \in [0,T]$. Using (18), the T-average growth rate is given by $(1-C)\gamma(I_M(y)) = \frac{K\sigma I_M(y)}{1+\tau\sigma I_M(y)+\frac{k_d}{k_r}\tau(\sigma I_M(y))^2} = \mu_S(I_M(y))$. For the high/low light regime, one has

$$C(y,t) = \begin{cases} \frac{\alpha_H(y)}{\alpha_H(y)+k_r}(1-e^{-(\alpha_H(y)+k_r)t}) + e^{-(\alpha_H(y)+k_r)t}C(y,0), & t \in (0,\eta T) \\ \frac{\alpha_L(y)}{\alpha_L(y)+k_r}(1-e^{-(\alpha_L(y)+k_r)(t-\eta T)}) + e^{-(\alpha_L(y)+k_r)(t-\eta T)}C(y,\eta T), & t \in (\eta T, T) \end{cases}$$

Using the periodic border condition of C, one has

$$C(y,0) = \frac{\frac{\alpha_L(y)}{\alpha_L(y)+k_r}\left(1-e^{-(\alpha_L(y)+k_r)T(1-\eta)}\right) + e^{-(\alpha_L(y)+k_r)T(1-\eta)}\frac{\alpha_H(y)}{\alpha_H(y)+k_r}\left(1-e^{-(\alpha_H(y)+k_r)T\eta}\right)}{1-e^{-(\alpha_L(y)+k_r)T(1-\eta)-(\alpha_H(y)+k_r)T\eta}}.$$

For a given local optical depth y, the T-average growth rate is given by

$$\begin{aligned}\bar{\mu}^{\mathrm{T}}(y) =& \frac{1}{T}\int_0^T \mu(y,t)\mathrm{d}t \\ =& \frac{1}{T}\Big(\int_0^{\eta T} \mu(y,t)\mathrm{d}t + \int_{\eta T}^{T} \mu(y,t)\mathrm{d}t\Big) \\ =& \eta\frac{\gamma_H(y)k_r}{\alpha_H(y)+k_r} + (1-\eta)\frac{\gamma_L(y)k_r}{\alpha_L(y)+k_r} \\ &+ \frac{\gamma_H(y)}{T(\alpha_H(y)+k_r)}\left(\frac{\alpha_H(y)}{\alpha_H(y)+k_r} - C(y,0)\right)\left(1-e^{-(\alpha_H(y)+k_r)T\eta}\right) \\ &+ \frac{\gamma_L(y)}{T(\alpha_L(y)+k_r)}\left(\frac{\alpha_L(y)}{\alpha_L(y)+k_r} - C(y,T\eta)\right)\left(1-e^{-(\alpha_L(y)+k_r)T(1-\eta)}\right) \\ =& \eta\mu_S(I_H(y)) + (1-\eta)\mu_S(I_L(y)) + \frac{\zeta_1(y,\eta,T)\zeta_2(y)}{Tk_r},\end{aligned}$$

where $\gamma_H(y) := \gamma(I_H(y))$ and $\gamma_L(y) := \gamma(I_L(y))$.

A.2 Case II: Small period T

For small period case, the dynamics of C is negligible (*i.e.* C is a constant). Integrating (7) from 0 to T gives

$$0 = \int_0^T \dot{C}\mathrm{d}t = -k_rTC - k_d\sigma C\int_0^T I\mathrm{d}t + k_d\sigma\int_0^T I\mathrm{d}t - k_d\sigma\int_0^T IA\mathrm{d}t.$$

Let us denote by $\bar{I} := \frac{1}{T}\int_0^T I\mathrm{d}t$ and by $\overline{IA} := \frac{1}{T}\int_0^T IA\mathrm{d}t$, then one finds the constant value for C as

$$C = \frac{k_d\sigma(\bar{I}-\overline{IA})}{k_d\sigma\bar{I}+k_r}. \tag{A1}$$

For high/low light regime, one has

$$A(y,t) = \begin{cases} e^{-\beta_H(y)t}A(0) + \frac{1-C}{\tau\beta_H(y)}(1-e^{-\beta_H(y)t}), & t\in[0,\eta T], \\ e^{-\beta_L(y)(t-\eta T)}A(\eta T) + \frac{1-C}{\tau\beta_L(y)}(1-e^{-\beta_L(y)(t-\eta T)}), & t\in[\eta T, T]. \end{cases}$$

The periodicity on A gives

$$A(y,0) = \frac{e^{-\beta_L(y)(1-\eta)T}\frac{1-C}{\tau\beta_H(y)}(1-e^{-\beta_H(y)\eta T}) + \frac{1-C}{\tau\beta_L(y)}(1-e^{-\beta_L(y)(1-\eta)T})}{1-e^{-\beta_L(y)(1-\eta)T-\beta_H(y)\eta T}}.$$

On the other hand, the average of IA can be computed by

$$
\begin{aligned}
T\overline{IA} =& \int_0^{\eta T} I_H(y)A(y,t)\mathrm{d}t + \int_{\eta T}^{T} I_L(y)A(y,t)\mathrm{d}t \\
=& A(y,0)I_H(y)\frac{1-e^{-\beta_H(y)\eta T}}{\beta_H(y)} + I_H(y)\frac{1-C}{\tau\beta_H(y)}(\eta T - \frac{1-e^{-\beta_H(y)\eta T}}{\beta_H(y)}) \\
&+ A(y,\eta T)I_L(y)\frac{1-e^{-\beta_L(y)(1-\eta)T}}{\beta_L(y)} + I_L(y)\frac{1-C}{\tau\beta_L(y)}\big((1-\eta)T \\
&- \frac{1-e^{-\beta_L(y)(1-\eta)T}}{\beta_L(y)}\big) \\
=& A(y,0)I_H(y)\frac{1-e^{-\beta_H(y)\eta T}}{\beta_H(y)} + I_H(y)\frac{1-C}{\tau\beta_H(y)}(\eta T - \frac{1-e^{-\beta_H(y)\eta T}}{\beta_H(y)}) \\
&+ \big(e^{-\beta_H(y)\eta T}A(0) + \frac{1-C}{\tau\beta_H(y)}(1-e^{-\beta_H(y)\eta T})\big)I_L(y)\frac{1-e^{-\beta_L(y)(1-\eta)T}}{\beta_L(y)} \\
&+ I_L(y)\frac{1-C}{\tau\beta_L(y)}\big((1-\eta)T - \frac{1-e^{-\beta_L(y)(1-\eta)T}}{\beta_L(y)}\big) \\
=& \frac{A(y,0)}{\beta_H(y)\beta_L(y)}\big(I_H(y)\beta_L(y)(1-e^{-\beta_H(y)\eta T}) + I_L(y)\beta_H(y)e^{-\beta_H(y)\eta T}(1 \\
&- e^{-\beta_L(y)(1-\eta)T})\big) + \frac{1-C}{\tau\beta_H(y)\beta_L(y)}(I_H(y)\beta_L(y)\eta T \\
&+ I_L(y)\beta_H(y)(1-\eta)T) + \frac{1-C}{\tau\beta_L(y)^2\beta_H(y)^2}\big(I_L(y)\beta_H(y)\beta_L(y)(1 \\
&- e^{-\beta_H(y)\eta T})(1-e^{-\beta_L(y)(1-\eta)T}) - I_H(y)\beta_L(y)^2(1-e^{-\beta_H(y)\eta T}) \\
&- I_L(y)\beta_H(y)^2(1-e^{-\beta_L(y)(1-\eta)T})\big) \\
=& \frac{1-C}{\tau\beta_L(y)^2\beta_H(y)^2}\frac{1}{1-e^{-\beta_L(y)(1-\eta)T-\beta_H(y)\eta T}}\big(I_H(y)\beta_L(y)^2(1 \\
&- e^{-\beta_H(y)\eta T})^2e^{-\beta_L(y)(1-\eta)T} + I_L(y)\beta_L(y)\beta_H(y)e^{-\beta_L(y)(1-\eta)T-\beta_H(y)\eta T}(1 \\
&- e^{-\beta_H(y)\eta T})(1-e^{-\beta_L(y)(1-\eta)T}) + I_H(y)\beta_L(y)\beta_H(y)(1 \\
&- e^{-\beta_H(y)\eta T})(1-e^{-\beta_L(y)(1-\eta)T}) + I_L(y)\beta_H(y)^2e^{-\beta_H(y)\eta T}(1 \\
&- e^{-\beta_L(y)(1-\eta)T})^2 + I_L(y)\beta_H(y)\beta_L(y)(1-e^{-\beta_H(y)\eta T})(1 \\
&- e^{-\beta_L(y)(1-\eta)T})(1-e^{-\beta_L(y)(1-\eta)T-\beta_H(y)\eta T}) - I_H(y)\beta_L(y)^2(1 \\
&- e^{-\beta_H(y)\eta T})(1-e^{-\beta_L(y)(1-\eta)T-\beta_H(y)\eta T}) - I_L(y)\beta_H(y)^2(1 \\
&- e^{-\beta_L(y)(1-\eta)T})(1-e^{-\beta_L(y)(1-\eta)T-\beta_H(y)\eta T})\big) \\
&+ \frac{1-C}{\tau\beta_H(y)\beta_L(y)}(I_H(y)\beta_L(y)\eta T + I_L(y)\beta_H(y)(1-\eta)T).
\end{aligned}
$$

To simplify the notations, let us denote by $a := -(\sigma I_{\max} + \frac{1}{\tau})\eta T$ and by $i := -(\sigma I_{\min} + \frac{1}{\tau})(1-\eta)T$, then $A(0) = \frac{1-C}{\tau\beta_L\beta_H(y)}\frac{1}{1-e^{a+i}}(\beta_L e^i(1-e^a) + \beta_L(1-e^i))$

and the previous computation can be written as (we omitted the dependence on y)

$$
\begin{aligned}
T\overline{IA} =& A(0)I_H\frac{1-e^a}{\beta_H} + I_H\frac{1-C}{\tau\beta_H}(\eta T - \frac{1-e^a}{\beta_H}) + e^a A(0)I_L\frac{1-e^i}{\beta_L}\\
&+ \frac{1-C}{\tau\beta_H}(1-e^a)I_L\frac{1-e^i}{\beta_L} + I_L\frac{1-C}{\tau\beta_L}((1-\eta)T - \frac{1-e^i}{\beta_L})\\
=& \frac{A(0)}{\beta_H\beta_L}(I_H\beta_H(1-e^a) + I_L\beta_L e^a(1-e^i)) + \frac{1-C}{\tau\beta_H\beta_L}(I_H\beta_L\eta T + I_L\beta_H(1-\eta)T)\\
&+ \frac{1-C}{\tau\beta_H^2\beta_L^2}\big(I_L\beta_H\beta_L(1-e^a)(1-e^i) - I_H\beta_L^2(1-e^a) - I_L\beta_H^2(1-e^i)\big)\\
=& \frac{1-C}{\tau\beta_H^2\beta_L^2}\frac{1}{1-e^{a+i}}\big(I_H\beta_L^2(1-e^a)^2e^i + I_L\beta_H\beta_L e^{a+i}(1-e^a)(1-e^i)\\
&+ I_H\beta_H\beta_L(1-e^a)(1-e^i) + I_L\beta_H^2 e^a(1-e^i)^2 + I_L\beta_H\beta_L(1-e^a)(1-e^i)(1-e^{a+i})\\
&- I_H\beta_L^2(1-e^a)(1-e^{a+i}) - I_L\beta_H^2(1-e^i)(1-e^{a+i})\big) + \frac{1-C}{\tau\beta_H\beta_L}(I_H\beta_L\eta T + I_L\beta_H(1-\eta)T)\\
=& \frac{1-C}{\tau\beta_H^2\beta_L^2}\frac{1}{1-e^{a+i}}\big(I_H\beta_L^2(1-e^a)(e^i-1) + I_H\beta_L^2(e^a-1)(1-e^i) + I_H\beta_L\beta_L(1-e^a)(1-e^i)\\
&+ I_H\beta_L\beta_L(1-e^a)(1-e^i)\big) + \frac{1-C}{\tau\beta_L\beta_L}(I_H\beta_L\eta T + I_H\beta_L(1-\eta)T)\\
=& \frac{1-C}{\tau\beta_L^2\beta_L^2}\frac{(1-e^a)(1-e^i)}{1-e^{a+i}}\big(I_H\beta_L\beta_L + I_H\beta_L\beta_L - I_H\beta_L^2 - I_H\beta_L^2\big)\\
&+ \frac{1-C}{\tau\beta_L\beta_L}(I_H\beta_L\eta T + I_H\beta_L(1-\eta)T)\\
=& \frac{1-C}{\tau\beta_L^2\beta_L^2}\frac{(1-e^a)(1-e^i)}{1-e^{a+i}}(I_H\beta_L - I_H\beta_L)(\beta_L - \beta_L) + \frac{1-C}{\tau\beta_L\beta_L}(I_H\beta_L\eta T + I_H\beta_L(1-\eta)T).
\end{aligned}
$$

By using the definition of $I_H, I_H, \beta_L, \beta_L$, one has $(I_H\beta_L - I_H\beta_L)(\beta_L - \beta_L) = \frac{\sigma}{\tau}(I_{\max} - I_{\min})^2$ and $I_H\beta_L\eta T + I_H\beta_L(1-\eta)T = (\frac{I_M}{\tau} + \sigma I_{\max}I_{\min})T$. Replacing C by (A1) in the previous equation gives

$$
T\overline{IA} = \frac{k_d\sigma\overline{IA} + k_r}{\tau\beta_L^2\beta_L^2(k_d\sigma I_\eta + k_r)}\Big(\Delta(y,T)\frac{\sigma}{\tau}(I_{\max} - I_{\min})^2 + (\frac{I_\eta}{\tau} + \sigma I_{\max}I_{\min})\beta_L\beta_L T\Big),
$$

where $\delta(y,T) = \frac{(1-e^a)(1-e^i)}{1-e^{a+i}}$. In other words

$$
\overline{IA} = \frac{k_r\Big(\frac{\Delta(y,T)}{T\beta_L\beta_L}\frac{\sigma}{\tau}(I_{\max} - I_{\min})^2 + \frac{I_\eta}{\tau} + \sigma I_{\max}I_{\min}\Big)}{\tau\beta_L\beta_L(k_d\sigma I_\eta + k_r) - k_d\sigma\Big(\frac{\Delta(y,T)}{T\beta_L\beta_L}\frac{\sigma}{\tau}(I_{\max} - I_{\min})^2 + \frac{I_\eta}{\tau} + \sigma I_{\max}I_{\min}\Big)}.
$$

We have that

$$
\Theta := \frac{\Delta(y,T)(1+\tau\sigma I_\eta(y))}{(1+\tau\sigma I_H(y))(1+\tau\sigma I_L(y))\eta(1-\eta)} \to 1 \text{ as } T \to 0,
$$

and we can manipulate the value $\overline{IA}$ to get

$$\overline{IA} = \frac{\frac{k_r I_\eta}{(1+\tau\sigma I_\eta)\beta_L\beta_L\tau^2}\left(\tau^2\beta_L\beta_L\right) + (\Theta-1)\tau\sigma(I_L-I_H)^2\eta(1-\eta)}{k_r + k_d\sigma I_\eta - k_d\sigma\frac{I_\eta}{(1+\tau\sigma)\tau^2\beta_L\beta_L}\left(\tau^2\beta_L\beta_L\right) + (\Theta-1)\tau\sigma(I_L-I_H)^2\eta(1-\eta)},$$

and rearranging this last equality, we get

$$\bar{\mu}^{\mathrm{T}}(y) = \frac{K\sigma k_r I_M(y)\big(1+\xi_1(y)\xi_2(y,T)\big)}{k_r + k_r\tau\sigma I_M(y) + k_d\tau\big(\sigma I_M(y)\big)^2 + k_d\sigma I_M(y)\xi_1(y)\xi_2(y,T)}, \quad \text{(A2)}$$

where

$$\xi_1(y) = \frac{\sigma\big(I_H(y)-I_L(y)\big)^2\eta(1-\eta)}{\tau\beta_H(y)\beta_L(y)},$$
$$\xi_2(y,T) = \frac{(1-e^{-\beta_H(y)\eta T})(1-e^{-\beta_L(y)(1-\eta)T})}{T(1-e^{-\beta_H(y)\eta T-\beta_L(y)(1-\eta)T})}\frac{\eta\beta_H(y)+(1-\eta)\beta_L(y)}{\eta(1-\eta)\beta_H(y)\beta_L(y)} - 1.$$

A.3 Proof of Lemma 1

We split equation (7) into the high/low-flashing light configuration

$$\begin{cases} \frac{\mathrm{d}}{dt}\begin{pmatrix}A(y,t)\\C(y,t)\end{pmatrix} = -M_H(y)\begin{pmatrix}A(y,t)\\C(y,t)\end{pmatrix} + N_H(y), \text{ if } t<\eta T,\\ \frac{\mathrm{d}}{\mathrm{d}t}\begin{pmatrix}A(y,t)\\C(y,t)\end{pmatrix} = -M_L(y)\begin{pmatrix}A(y,t)\\C(y,t)\end{pmatrix} + N_L(y), \text{ if } t>\eta T. \end{cases}$$

One can solve this system by using the variation of parameters method and get

$$\begin{pmatrix}A(y,t)\\C(y,t)\end{pmatrix} = \left(\mathrm{Id}-e^{-tM_H(y)}\right)M_H^{-1}(y)N_H(y) + e^{-tM_H(y)}\begin{pmatrix}A(y,0)\\C(y,0)\end{pmatrix}, \quad \text{if } t<\eta T,$$
$$\begin{pmatrix}A(y,t)\\C(y,t)\end{pmatrix} = \left(\mathrm{Id}-e^{-(t-\eta T)M_L(y)}\right)M_L^{-1}(y)N_L(y) + e^{-(t-\eta T)M_L(y)}\begin{pmatrix}A(y,\eta T)\\C(y,\eta T)\end{pmatrix}, \text{ if } t>\eta T,$$

where Id denotes the identity matrix in $\mathbb{R}^{2\times 2}$. Imposing then periodic conditions, i.e, $(A(y,0),C(y,0)) = (A(y,T),C(y,T))$, one can evaluate the values of $(A(y,0),C(y,0))$ and $(A(y,\eta T),C(y,\eta T))$:

$$\begin{pmatrix} A(y,\eta T) \\ C(y,\eta T) \end{pmatrix} = \left(\mathrm{Id} - e^{-\eta T M_H(y)}\right) M_H^{-1}(y) N_H(y) + e^{-\eta T M_H(y)} \begin{pmatrix} A(y,0) \\ C(y,0) \end{pmatrix}, \tag{A3}$$

$$\begin{pmatrix} A(y,0) \\ C(y,0) \end{pmatrix} = \left(\mathrm{Id} - e^{-(1-\eta) T M_L(y)}\right) M_L^{-1}(y) N_L(y) + e^{-(1-\eta) T M_L(y)} \begin{pmatrix} A(y,\eta T) \\ C(y,\eta T) \end{pmatrix}. \tag{A4}$$

Replacing finally (A4) in (A3) and vice versa, we obtain

$$\begin{aligned} \begin{pmatrix} A(y,\eta T) \\ C(y,\eta T) \end{pmatrix} = & \left(\mathrm{Id} - e^{-\eta T M_H(y)} e^{-(1-\eta) T M_L(y)}\right)^{-1} \\ & \cdot \left[\left(\mathrm{Id} - e^{-\eta T M_H(y)}\right) M_H^{-1}(y) N_H(y) \right. \\ & \left. + e^{-\eta T M_H(y)} \left(\mathrm{Id} - e^{-(1-\eta) T M_L(y)}\right) M_L^{-1}(y) N_L(y) \right], \end{aligned} \tag{A5}$$

$$\begin{aligned} \begin{pmatrix} A(y,0) \\ C(y,0) \end{pmatrix} = & \left(\mathrm{Id} - e^{-(1-\eta) T M_L(y)} e^{-\eta T M_H(y)}\right)^{-1} \\ & \cdot \left[\left(\mathrm{Id} - e^{-(1-\eta) T M_L(y)}\right) M_L^{-1}(y) N_L(y) \right. \\ & \left. + e^{-(1-\eta) T M_L(y)} \left(\mathrm{Id} - e^{-\eta T M_H(y)}\right) M_H^{-1}(y) N_H(y) \right]. \end{aligned} \tag{A6}$$

The inverse matrix $(Id - e^{-\eta T M_H} e^{-(1-\eta) T M_L})$ exists because the matrix $e^{-\eta T M_H} e^{-(1-\eta) T M_L}$ has no eigenvalue equal to 1. The solution founded it is then unique.

A.4 Exact growth rate

To calculate the T-average of the growth rate, we calculate the integral $\int_0^T I(y,t)(A(y,t), C(y,t))dt$:

$$\begin{aligned} \int_0^T I(y,t) \begin{pmatrix} A(y,t) \\ C(y,t) \end{pmatrix} dt = & I_H(y) \int_0^{\eta T} \begin{pmatrix} A(y,t) \\ C(y,t) \end{pmatrix} dt + I_L(y) \int_{\eta T}^T \begin{pmatrix} A(y,t) \\ C(y,t) \end{pmatrix} dt \\ = & \eta T I_H(y) M_H^{-1}(y) N_H(y) \\ & - I_H(y) M_H^{-1}(y) \left(\mathrm{Id} - e^{-\eta T M_H(y)}\right) \left[M_H^{-1}(y) N_H(y) - \begin{pmatrix} A(y,0) \\ C(y,0) \end{pmatrix} \right] \\ & + I_L(y)(1-\eta) T M_L^{-1}(y) N_L(y) \\ & - I_L(y) M_L^{-1}(y) \left(\mathrm{Id} - e^{-(1-\eta) T M_L(y)}\right) \left[M_L^{-1}(y) N_L(y) - \begin{pmatrix} A(y,\eta T) \\ C(y,\eta T) \end{pmatrix} \right]. \end{aligned} \tag{A7}$$

Using (A5) we can compute

$$M_L^{-1}(y) N_L(y) - \begin{pmatrix} A(y,\eta T) \\ C(y,\eta T) \end{pmatrix}$$

$$
\begin{aligned}
&= M_L^{-1}(y)N_L(y) - \left(\mathrm{Id} - e^{-\eta T M_H(y)} e^{-(1-\eta)TM_L(y)}\right)^{-1} \\
&\quad \cdot \left[\left(\mathrm{Id} - e^{-\eta T M_H(y)}\right) M_H^{-1}(y)N_H(y)\right. \\
&\qquad \left. + e^{-\eta T M_H(y)} \left(\mathrm{Id} - e^{-(1-\eta)TM_L(y)}\right) M_L^{-1}(y)N_L(y)\right] \\
&= \left(\mathrm{Id} - e^{-\eta T M_H(y)} e^{-(1-\eta)TM_L(y)}\right)^{-1} \\
&\quad \cdot \left[(\mathrm{Id} - e^{-\eta T M_H(y)}) M_L^{-1}(y)N_L(y) - (\mathrm{Id} - e^{-\eta T M_H(y)}) M_H^{-1}(y)N_H(y)\right. \\
&\quad \left. - e^{-\eta T M_H(y)} (\mathrm{Id} - e^{-(1-\eta)TM_H(y)}) M_L^{-1}(y)N_L(y)\right] \\
&= \left(\mathrm{Id} - e^{-\eta T M_H(y)} e^{-(1-\eta)TM_L(y)}\right)^{-1} \left[M_L^{-1}(y)N_L(y)\right. \\
&\quad - e^{-\eta T M_H(y)} e^{-(1-\eta)TM_L(y)} M_L^{-1}(y)N_L(y) - M_H^{-1}(y)N_H(y) \\
&\quad + e^{-\eta T M_H(y)} M_H^{-1}(y)N_H(y) - e^{-\eta T M_H(y)} M_L^{-1}(y)N_L(y) \\
&\quad \left. + e^{-e\eta T M_H(y)} e^{-(1-\eta)TM_L(y)} M_L^{-1} N_L(y)\right] \\
&= \left(\mathrm{Id} - e^{-\eta T M_H(y)} e^{-(1-\eta)TM_L(y)}\right)^{-1} \left[(\mathrm{Id} - e^{-\eta T M_H(y)}) M_L^{-1}(y)N_L(y)\right. \\
&\quad \left. - (\mathrm{Id} - e^{-\eta T M_H(y)}) M_H^{-1}(y)N_H(y)\right] \\
&= \left(\mathrm{Id} - e^{-\eta T M_H(y)} e^{-(1-\eta)TM_L(y)}\right)^{-1} \cdot \\
&(\mathrm{Id} - e^{-\eta T M_H(y)})(M_L^{-1}(y)N_L(y) - M_H^{-1}(y)N_H(y)).
\end{aligned}
$$

In the same way, using (A6) we can get

$$
\begin{aligned}
M_H^{-1}(y)N_H(y) - \begin{pmatrix} A(y,0) \\ C(y,0) \end{pmatrix} &= \left(\mathrm{Id} - e^{-(1-\eta)TM_L(y)} e^{-\eta T M_H(y)}\right)^{-1} (\mathrm{Id} - e^{-(1-\eta)TM_L(y)}) \\
&\cdot (M_H^{-1} N_H(y) - M_L^{-1} N_L(y)).
\end{aligned}
$$

Replacing the above calculations on (A7), we have

$$
\int_0^T I(y,t) \begin{pmatrix} A(y,t) \\ C(y,t) \end{pmatrix} = \eta T I_H(y) M_H^{-1}(y) N_H(y) + (1-\eta) T I_L(y) M_L^{-1}(y) N_L(y) + \Delta, \tag{A8}
$$

where

$$
\begin{aligned}
\Delta = \Bigg[& I_H(y) M_H^{-1}(y) \left(\mathrm{Id} - e^{-\eta T M_H(y)}\right) \left(\mathrm{Id} - e^{-(1-\eta)TM_L(y)} e^{-\eta T M_H(y)}\right)^{-1} \left(\mathrm{Id} - e^{-(1-\eta)TM_L(y}\right) \\
& - I_L(y) M_L^{-1}(y) \left(\mathrm{Id} - e^{-(1-\eta)TM_L(y}\right) \left(\mathrm{Id} - e^{-\eta T M_H(y)} e^{-(1-\eta)TM_L(y)}\right)^{-1} \left(\mathrm{Id} - e^{-\eta T M_H(y)}\right) \Bigg] \\
& \cdot \left(M_H^{-1}(y)N_H(y) - M_L^{-1}(y)N_L(y)\right).
\end{aligned}
$$

Finally, the average growth rate $\frac{1}{T}\int_0^T K\sigma I A dt$ is proportional to the first coordinate of (A8) multiplied by $\frac{K\sigma}{T}$. Denote δ the first coordinate of Δ and note that

$$M_H^{-1}(y)N_H(y) = \begin{pmatrix} \dfrac{k_r}{\tau k_d(\sigma I_H(y))^2 + \tau k_r \sigma I_H(y) + k_r} \\ \dfrac{\tau k_d(\sigma I_H(y))^2}{\tau k_d(\sigma I_H(y))^2 + \tau k_r \sigma I_H(y) + k_r} \end{pmatrix}, \tag{A9}$$

$$M_L^{-1}(y)N_L(y) = \begin{pmatrix} \dfrac{k_r}{\tau k_d(\sigma I_L(y))^2 + \tau k_r \sigma I_L(y) + k_r} \\ \dfrac{\tau k_d(\sigma I_L(y))^2}{\tau k_d(\sigma I_L(y))^2 + \tau k_r \sigma I_L(y) + k_r} \end{pmatrix}, \tag{A10}$$

where the first coordinate in (A9) and (A10) multiplied by $K\sigma$ is exactly $\mu_S(I_H(y))$ and $\mu_S(I_L(y))$ respectively. So, the T-average of the growth rate is

$$\bar{\mu}^{\mathrm{T}}(y) = \eta\mu_s(I_H(y)) + (1-\eta)\mu_S(I_L(y)) - \frac{K\sigma}{T}\delta(y,T). \tag{A11}$$

A.5 Eigenvalues of matrix M

We will condense the analysis of the eigenvalues of M_H and M_L in the matrix

$$M(I) = \begin{pmatrix} \sigma I + \frac{1}{\tau} & \frac{1}{\tau} \\ k_d\sigma I & k_d\sigma I + k_r \end{pmatrix}.$$

Denoting λ_1 and λ_2 the eigenvalues, then we have

$$\mathrm{Tr}(M(I)) = \lambda_1 + \lambda_2 = \sigma I + \frac{1}{\tau} + k_d\sigma I + k_r, \tag{A12}$$

$$\mathrm{Det}(M(I)) = \lambda_1\lambda_2 = k_d(\sigma I)^2 + k_r\sigma I + \frac{k_r}{\tau}. \tag{A13}$$

From (A13), λ_1 and λ_2 has the same sign, and since (A12) holds, the two eigenvalues are positive.

Appendix B Proof of Lemma 3

The second derivative of the function μ_S can be computed as

$$\frac{\mathrm{d}^2}{\mathrm{d}I^2}\mu_S(I) = -\frac{2K\sigma\left[\tau\sigma + \frac{k_d}{k_r}\tau\sigma^2 I\left(3 - \frac{k_d}{k_r}\tau\sigma^2 I^2\right)\right]}{\left(1 + \tau\sigma I + \frac{k_d}{k_r}\tau(\sigma I)^2\right)^3},$$

and it is zero in the point I_c which satisfies

$$\left(\frac{k_d}{k_r}\tau\sigma^2\right)^2 I_c^3 - 3\frac{k_d}{k_r}\tau\sigma^2 I_c - \tau\sigma = 0.$$

This is a depressed cubic equation, where the determinant correspond to

$$\Delta = \left(\frac{1}{\frac{k_d}{k_r}\tau\sigma^2}\right)^4 (\tau\sigma)^2 - 4\left(\frac{1}{\frac{k_d}{k_r}\tau\sigma^2}\right)^3$$

where if $\Delta \leq 0$ all the roots are real. Note that

$$\Delta \leq 0 \iff \tau \leq 4\frac{k_d}{k_r}.$$

In this case, the solutions are given by (Zwillinger, 2018):

$$l\cos\frac{\theta}{3}, \quad l\cos\frac{\theta+2\pi}{3}, \quad \text{and} \quad l\cos\frac{\theta+4\pi}{3}$$

where

$$l = \frac{2}{\sigma\sqrt{\frac{k_d}{k_r}\tau}}, \quad \text{and} \quad \theta = \arccos\left(\frac{\sqrt{\tau}}{2\sqrt{\frac{k_d}{k_r}}}\right).$$

From the three possible solutions, only $l\cos\frac{\theta}{3}$ is positive due to $\theta/3 \in (0, \pi/6)$. In the case that $\Delta > 0$ then the real solution can be written as (Holmes, 2002)

$$l\cosh\left(\frac{1}{3}\operatorname{arccosh}\left(\frac{\sqrt{\tau}}{2\sqrt{\frac{k_d}{k_r}}}\right)\right).$$

References

Abu-Ghosh S, Fixler D, Dubinsky Z, et al (2015a) Continuous background light significantly increases flashing-light enhancement of photosynthesis and growth of microalgae. Bioresource technology 187:144–148

Abu-Ghosh S, Fixler D, Dubinsky Z, et al (2015b) Flashing light enhancement of photosynthesis and growth occurs when photochemistry and photoprotection are balanced in dunaliella salina. European Journal of Phycology 50(4):469–480. https://doi.org/10.1080/09670262.2015.1069404, URL https://doi.org/10.1080/09670262.2015.1069404, https://arxiv.org/abs/https://doi.org/10.1080/09670262.2015.1069404

Abu-Ghosh S, Fixler D, Dubinsky Z, et al (2016) Flashing light in microalgae biotechnology. Bioresource Technology 203:357–363. https://doi.org/https://doi.org/10.1016/j.biortech.2015.12.057, URL https://www.sciencedirect.com/science/article/pii/S0960852415016879

Baklouti M, Faure V, Pawlowski L, et al (2006) Investigation and sensitivity analysis of a mechanistic phytoplankton model implemented in a new modular numerical tool (eco3m) dedicated to biogeochemical modelling. Progress in Oceanography 71(1):34–58. https://doi.org/https://doi.org/10.1016/j.pocean.2006.05.003, URL https://www.sciencedirect.com/science/article/pii/S0079661106000772

Balamurugan S, Sathishkumar R, Li HY (2021) Biotechnological perspectives to augment the synthesis of valuable biomolecules from microalgae by employing wastewater. Journal of Water Process Engineering 39:101,713

Béchet Q, Shilton A, Guieysse B (2013) Modeling the effects of light and temperature on algae growth: state of the art and critical assessment for productivity prediction during outdoor cultivation. Biotechnology advances 31(8):1648–1663

Bernard O, Lu LD (2021) Optimal optical conditions for Microalgal production in photobioreactors, URL https://hal.archives-ouvertes.fr/hal-03323094, submitted paper

Bernard O, Mairet F, Chachuat B (2015) Modelling of microalgae culture systems with applications to control and optimization. Microalgae Biotechnology pp 59–87

Combe C, Hartmann P, Rabouille S, et al (2015) Long-term adaptive response to high-frequency light signals in the unicellular photosynthetic eukaryote dunaliella salina. Biotechnology and Bioengineering 112(6):1111–1121

Demory D, Combe C, Hartmann P, et al (2018) How do microalgae perceive light in a high-rate pond? towards more realistic lagranbookgian experiments. Royal Society open science 5(5):180,523

Fernández-Sevilla JM, Brindley C, Jiménez-Ruíz N, et al (2018) A simple equation to quantify the effect of frequency of light/dark cycles on the photosynthetic response of microalgae under intermittent light. Algal Research 35:479–487. https://doi.org/https://doi.org/10.1016/j.algal.2018.09.026, URL https://www.sciencedirect.com/science/article/pii/S2211926417308937

Grenier J, Lopes F, Bonnefond H, et al (2020) Worldwide perspectives of rotating algal biofilm up-scaling, submitted paper

Han BP (2002) A mechanistic model of algal photoinhibition induced by photodamage to photosystem-ii. Journal of Theoretical Biology 214(4):519–527. https://doi.org/https://doi.org/10.1006/jtbi.2001.2468, URL https://www.sciencedirect.com/science/article/pii/S0022519301924683

Hartmann P, Béchet Q, Bernard O (2014) The effect of photosynthesis time scales on microalgae productivity. Bioprocess and biosystems engineering 37(1):17–25

Holmes G (2002) The use of hyperbolic cosines in solving cubic polynomials. The Mathematical Gazette 86(507):473–477

Khalil H (2002) Nonlinear Systems. Pearson Education, Prentice Hall, URL https://books.google.fr/books?id=t_d1QgAACAAJ

Lamare PO, Aguillon N, Sainte-Marie J, et al (2019) Gradient-based optimization of a rotating algal biofilm process. Automatica 105:80–88. https://doi.org/https://doi.org/10.1016/j.automatica.2019.02.043, URL https://www.sciencedirect.com/science/article/pii/S0005109819300974

Lu LD (2021) Lagrangian approach for modelling and optimization of coupled hydrodynamics-photosynthesis. Theses, Sorbonne Université, URL https://tel.archives-ouvertes.fr/tel-03625562

Milledge JJ (2011) Commercial application of microalgae other than as biofuels: a brief review. Reviews in Environmental Science and Bio/Technology 10(1):31–41

Morel A (1988) Optical modeling of the upper ocean in relation to its biogenous matter content (case i waters). Journal of geophysical research: oceans 93(C9):10,749–10,768

Nikolaou A, Bernardi A, Meneghesso A, et al (2015) A model of chlorophyll fluorescence in microalgae integrating photoproduction, photoinhibition and photoregulation. Journal of Biotechnology 194:91–99. https://doi.org/https://doi.org/10.1016/j.jbiotec.2014.12.001, URL https://www.sciencedirect.com/science/article/pii/S0168165614010323

Nikolaou A, Hartmann P, Sciandra A, et al (2016) Dynamic coupling of photoacclimation and photoinhibition in a model of microalgae growth. Journal of theoretical biology 390:61–72

Pozzobon V, Perre P (2018) Han's model parameters for microalgae grown under intermittent illumination: Determined using particle swarm optimization. Journal of Theoretical Biology 437:29–35. https://doi.org/https://doi.org/10.1016/j.jtbi.2017.10.010, URL https://www.sciencedirect.com/science/article/pii/S0022519317304733

Prasil O, Adir N, Ohad I (1992) Dynamics of photosystem ii: mechanism of photoinhibition and recovery process. Topics in photosynthesis 11:295–348

Raven JA (2011) The cost of photoinhibition. Physiologia plantarum 142(1):87–104

Sanders JA, Verhulst F, Murdock J (2007) Averaging Methods in Nonlinear Dynamical Systems, 2nd edn. Applied Mathematical Sciences, Springer-Verlag New York, https://doi.org/10.1007/978-0-387-48918-6

Schulze PS, Brindley C, Fernández JM, et al (2020) Flashing light does not improve photosynthetic performance and growth of green microalgae. Bioresource Technology Reports 9:100,367

Stramski D, Sciandra A, Claustre H (2002) Effects of temperature, nitrogen, and light limitation on the optical properties of the marine diatom thalassiosira pseudonana. Limnology and Oceanography 47(2):392–403

Wu X, Merchuk JC (2001) A model integrating fluid dynamics in photosynthesis and photoinhibition processes. Chemical Engineering Science 56(11):3527–3538. https://doi.org/https://doi.org/10.1016/S0009-2509(01)00048-3, URL https://www.sciencedirect.com/science/article/pii/S0009250901000483

Zwillinger D (2018) CRC standard mathematical tables and formulas. chapman and hall/CRC